A PHOTOGRAPHIC INVESTIGATION OF BUBBLE NUCLEATION CHARACTERISTICS

by

Roger Lee Sowersby

United States
Naval Postgraduate School

THESIS

A PHOTOGRAPHIC INVESTIGATION OF
BUBBLE NUCLEATION CHARACTERISTICS

by

Roger Lee Sowersby

December 1969

A Photographic Investigation of Bubble Nucleation Characteristics

by

Roger Lee Sowersby
Lieutenant, United States Navy
B.S., University of Southern California, 1963

Submitted in partial fulfillment of the
requirements for the degree of

MASTER OF SCIENCE IN MECHANICAL ENGINEERING

from the

NAVAL POSTGRADUATE SCHOOL
December 1969

ABSTRACT

The characteristics of bubble nucleation, growth, and departure during nucleate boiling were investigated. The liquid-vapor interface motion was analyzed using high speed motion picture photography. The fluids used were: distilled water, water with wetting agent, water with sucrose, ethanol, and freon-11. Cylindrical, conical, and reentrant cavity geometries were employed in addition to J, L, and I shaped capillaries. Cavity inner diameters were fixed at 0.085 centimeters and cavity depth ranged from 0.230 to 0.703 centimeters.

Consistent results were obtained for geometrically similar cavities and for the same cavity at different occasions. A thin liquid film was observed on the cavity inner wall which was directly related to cavity nucleation stability. The liquid-vapor interface penetration was shown to be dependent upon cavity geometry and fluid properties. Frequency, but not penetration, was affected by heat flux and superheat.

TABLE OF CONTENTS

LIST OF TABLES

LIST OF ILLUSTRATIONS

TABLE OF SYMBOLS

f	Bubble frequency, equal to $1/(t_d + t_g)$
h_{fg}	Latent heat of vaporization
l	Extension distance, equal to $(x^* + y^*)$
L	Overall depth of cavity
n_d	Number of frames from bubble departure to the end of dead time (interface reaches mouth of cavity)
n_g	Number of frames from end of dead time until departure
p	Pressure
p_l	Liquid pressure
p_v	Vapor pressure
r	Cavity radius
R	Universal gas constant
t	Time
t_d	Dead time, time from bubble departure for the interface to grow to the cavity mouth
t_g	Growth time, time from the end of dead time until bubble departure
T	Temperature
T_l	Bulk liquid temperature
T_s	Liquid saturation temperature
T_v	Vapor temperature
ΔT	Liquid superheat, equal to $(T_l - T_s)$
$x(t)$	Liquid-vapor interface penetration distance into a cavity

x^* Maximum interface penetration into a cavity

$\underline{x}^*$ Deviation from maximum penetration

y Distance from cavity mouth to thinnest part of vapor neck

y^* Breakoff distance, distance from cavity mouth to separation point of vapor bubble

v_l Specific volume of liquid

v_v Specific volume of vapor

α Breakoff angle

θ Contact angle

σ Surface tension

ACKNOWLEDGMENTS

The author would like to express his thanks to Dr. Paul J. Marto of the Naval Postgraduate School for his beneficial assistance, helpful suggestions, and enthusiastic support during the course of this study.

Thanks also to Mr. Robert C. Sheile, also of the Naval Postgraduate School, who manufactured laboratory apparatus and demonstrated skillful techniques and procedures during the construction of the glass cavities.

The Photographic Department, Pacific Missle Range, Point Mugu, contributed a great deal by developing all the films analyzed for this study. Their assistance in filming techniques also aided toward successful completion of this work.

I. INTRODUCTION

A. BACKGROUND AND THEORY

In the process of nucleate boiling, vapor bubbles form from entrapped gas or vapor within minute cavities, or nuclei, on the solid surface. These locations are called active sites. The subsequent growth and motion of these bubbles agitate the liquid and cause convection currents producing high heat transfer rates. Thus the importance of this mode of boiling becomes apparent.

Both theoretical as well as experimental work have shown the significant influence that surface cavities have upon nucleate boiling characteristics. It still remains unknown, however, what makes some cavities active and others inactive (where it is presumed that liquid fills up the cavity, displacing all the vapor or gas). One theory is that an active nucleating cavity becomes inactive by liquid rushing in behind a departing bubble, reaching the bottom of the cavity, filling and deactivating it.

Bankoff (Ref.2) developed an approximate theory for predicting the penetration distance for a cylindrical cavity. Neglecting inertial effects, he assumed that immediately after the disengagement of a bubble, the liquid-vapor meniscus is at equilibrium at the mouth of the cavity. Also, the temperature of the meniscus was taken to be equal to the saturation temperature of the liquid. The result obtained is simply $x = At^{\frac{1}{2}}$. His analysis provides as

time increased, penetration also increases. This model however, does not provide a mechanism for subsequent bubble growth. In effect, after departure of one bubble, all cavities should fill completely with liquid and deactivate.

In the theory of Marto and Rohsenow (Ref.10), inertial forces and viscous effects are both neglected and penetration is due only to capillary attraction. An imaginary volumetric heat source is used within the inrushing liquid to include the effect of heat transferred from the cavity walls. The resulting penetration as a function of time is: $x = Bt^{\frac{1}{2}} - Ct$ where the first term is similar to the proposal of Bankoff. Here, the wall conduction effect is included and yields the second term on the right hand side, missing in Bankoff's result. The interface penetration in this theory, goes to a maximum value, at which point the interface stops and its direction is reversed. During neckdown of the vapor, as a result of buoyant, surface tension, pressure, and inertial forces, interface motion begins into the cavity. This theory neglects the effects of viscous and inertia forces and obtains an initial velocity of infinity for the motion of the interface. Thus this model does not serve adequately at the beginning of interface motion but may represent very satisfactorily actual penetration after motion has commenced within the cavity when inertia and viscous effects become negligible in relation to other effects.

An early photographic study made concerning bubble formation characteristics was done by Prof. L. Trefethen (Ref.11). He illustrated a cleaned boiler being heated so that bubble columns rose from only a few sites on the glass surface. Each nucleation site was seen to be a continuous source of bubbles. In another experiment an artificial cavity was lowered into the superheated layer of water on the beaker bottom. Bubbles emerged continuously from the cavity until the cavity was raised into the cooler water. Here the vapor within the cavity partially condensed and no bubbles were formed until the cavity was again lowered to the bottom. A third experiment showed a roughened end of a glass rod being lowered into beer, supersaturated with carbon dioxide. The rough glass surface containing numerous vapor pockets, enabled the carbon dioxide to come out of solution rapidly, causing great bubble activity.

In a high speed motion picture study conducted with an individual cavity in water, Wei and Preckshot (Ref.12) obtained necking down and liquid-vapor interface motion data using 0.15, 0.07, and 0.01 centimeters I.D. glass capillary nucleation sites. They observed that a residual pocket of vapor remained in the site after a bubble departed, which grew to produce the next bubble. Photographs showed a liquid film remaining between the capillary mouth and the bubble surface after the bubble grew out of the capillary. It was shown that the necking down of the bubble

due to hydrodynamic and buoyant forces resulted in the interface attachment with the wall to proceed within the cavity. The residual vapor left in the cavity after bubble departure, they concluded, was related to the position of breakoff of the bubble neck which depended on cavity geometry.

Kosky (Ref.9) used a platinum filament imbedded in glass tubing to supply a heat flux to a 0.01 cm I.D. glass capillary of 2.0 cm depth. Bubble waiting period and growth time, average diameter of bubble at departure, and maximum penetration measurements were obtained. Motion of the interface was shown by a graph of penetration into the cavity versus time. He found that, for saturated boiling, the mechanism of bubble growth on the surface changed from inertia controlled at low pressures (20 mm) to surface tension controlled as the pressure increased to greater than 0.5 atmospheres. Particularly interesting were photographs of low pressure bubbles spread out across the surface, trapping a liquid microlayer under the bubble base, while the surface tension controlled bubbles remained spherical. Penetration obtained by visual measurements was less than 0.005 cm for a pressure of 20 mm and 0.05 cm penetration at 1.0 atmosphere.

Bubble growth occurring after the depressurization of distilled water in a glass tube was also investigated by Kosky (Ref.8). High speed films of the growth and elongation of spherical vapor bubbles due to restraining walls showed a thin film of liquid adhering to the wall which

greatly increased the vapor growth rate. Bubble growth equations were derived on one basic assumption that either (a) a liquid film adhered to the wall or (b) no liquid film existed and bubble growth was due to evaporation from the hemispherical ends only. Curves relating vapor growth as a function of time were obtained experimentally and followed extremely closely the equation derived with the assumption of the liquid film being present.

Bubble growth from an artificial glass cavity was investigated by DuBois (Ref.4). Photographs were shown of liquid slugs occurring as a result of liquid flowing down the walls, joining together, then being forced out by vaporization at the lower meniscus. DuBois compared growth and departure from a 0.10 cm. cylindrical cavity in glass to that from a cavity of the same size in a copper disk. Results obtained were in good agreement and he deduced that the same mechanism for bubble growth operated in both cavities. Thus, he showed that glass cavities serve as good models for nucleation in actual boiling surfaces. Penetration distances were also obtained in various fluids, but no penetration was observed in either water or water plus wetting agent. He theorized that this was caused by poor wetting of the glass cavities by the fluid. Cavity depth was not maintained constant, however, increasing the uncertainty in his experimental results.

Bubble growth along with departure diameter was studied by Eller (Ref.6). Contact angle and interface

penetration measurements were made. A detailed cleaning procedure was developed, using a hot chromic-sulphuric acid solution, to compare penetration results with values obtained by DuBois. Penetration in water, water with wetting agent, and ethanol was observed experimentally, but Eller's cavities also had variable depths, leading again to the uncertainty of results.

A pressure surge was also considered as a mechanism to disrupt or deactivate a nucleating cavity. In a study by Jameson and Kupferberg (Ref.7), the pressure fluctuation due to a spherical bubble moving from rest in an infinite fluid under the action of buoyant forces was analyzed. An equation was derived for the pressure change at the rest point, which is the point of contact of the bubble with the flat surface. A basic assumption was to neglect viscosity since the bubble began from rest. The derived pressure equation was plotted for nondimensional distance, the distance from the center of the bubble to the rest point divided by the bubble radius. This plot showed that the rest point was acted upon by a short pressure decrement which rapidly built up to a pressure excess and decreased to zero in an exponential manner. The maximum pressure excess occurred when the center of the bubble was one diameter from the rest point. Although the assumptions made in the beginning begin to break down in the region of 1.65 for the distance ratio, the pressure trend has already been established.

B. THESIS OBJECTIVES

The purpose of this thesis was to investigate stability considerations of a nucleation site by observing the liquid-vapor interface motion within prepared glass cavities. High speed motion pictures were to be used as a means of achieving this objective. Cavity configuration and fluid properties were to be varied in order to determine their effect on interface motion.

II. DESCRIPTION OF EXPERIMENTAL EQUIPMENT AND PROCEDURE

A. EQUIPMENT

Eleven models of nucleation cavities were constructed from Pyrex tubing and their properties are listed in Table 1. Dimensions were obtained by using a Gaertner Comparator. Appendix A describes procedures followed in cavity construction. (See Figs. 1 and 2.)

Three boilers, two constructed from 57 mm. Pyrex tubing and one from 80 mm. Pyrex tubing, were used during the experimental runs. A flat window was located just above the base of each boiler. The window diameter was 51 mm. in each case. A rubber stopper was used to mount the artificial cavities, two temperature probes, condenser, and to provide an airtight seal for the vacuum runs. A photograph of one boiler with cavity and probes mounted is presented in Fig.3. Cold tap water was circulated through the 14 inch long condenser to maintain a constant liquid level in the boiler. The condenser was held by two clamps to an iron stand.

A Bunsen burner was used to provide heat energy. A 6 inch iron ring, covered by a metal screen with an asbestos layer, was mounted on another iron stand. The ring assembly supported the boiler, rubber stopper and condenser.

Temperature measurements were accomplished by using a Hewlett Packard, Model 2801A, Quartz Thermometer and two

TABLE 1

PROPERTIES OF NUCLEATION CAVITIES

Cavity	Description	ID(cm)	OD(cm)	L(cm)	L/ID
G-2	Cylindrical, Short	0.0839	0.1526	0.2423	2.89
G-8	Cylindrical, Short	0.0838	0.1510	0.2401	2.86
8	Cylindrical, Short	0.0852	0.1555	0.2357	2.76
10	Cylindrical, Short	0.0846	0.1560	0.2298	2.72
43	Cylindrical, Medium	0.0854	0.1558	0.4400	5.15
52	Cylindrical, Long	0.0841	0.1524	0.7032	8.36
4	Conical	0.0830	0.2533	0.2360	2.84
Z	Reentrant	0.0851	0.2835	0.2581	3.04
24	Cylindrical-Reentrant	0.0609	0.3002	0.6633	10.9
K	Cylindrical	0.0578	0.2839	0.6507	11.3
32	Cylindrical with heater	0.0862	0.7230	0.2503	2.91
	Accuracy	$\pm$.0010	$\pm$.0010	$\pm$.0030	

Capillary Shapes

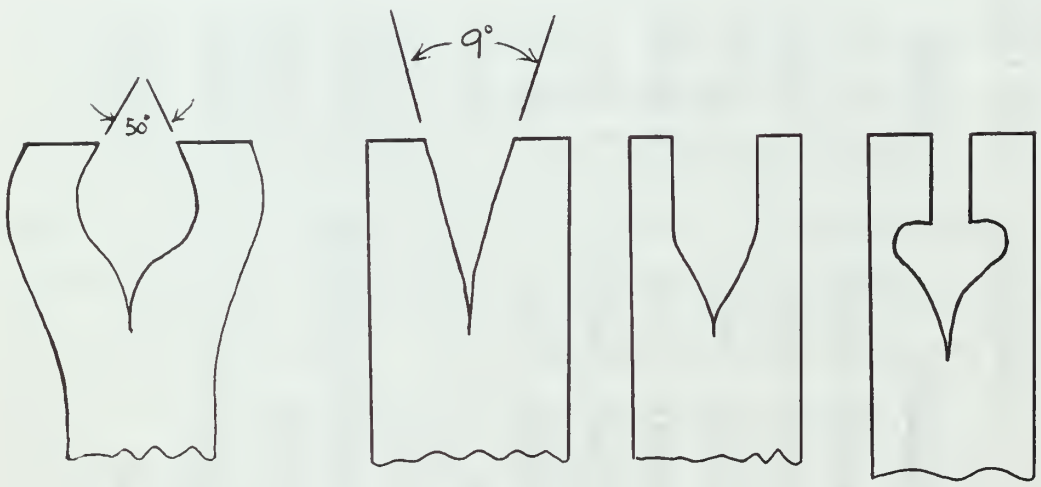

Cavity Internal Geometries

Fig. 1. - Capillary Shapes and Cavity Internal Geometries

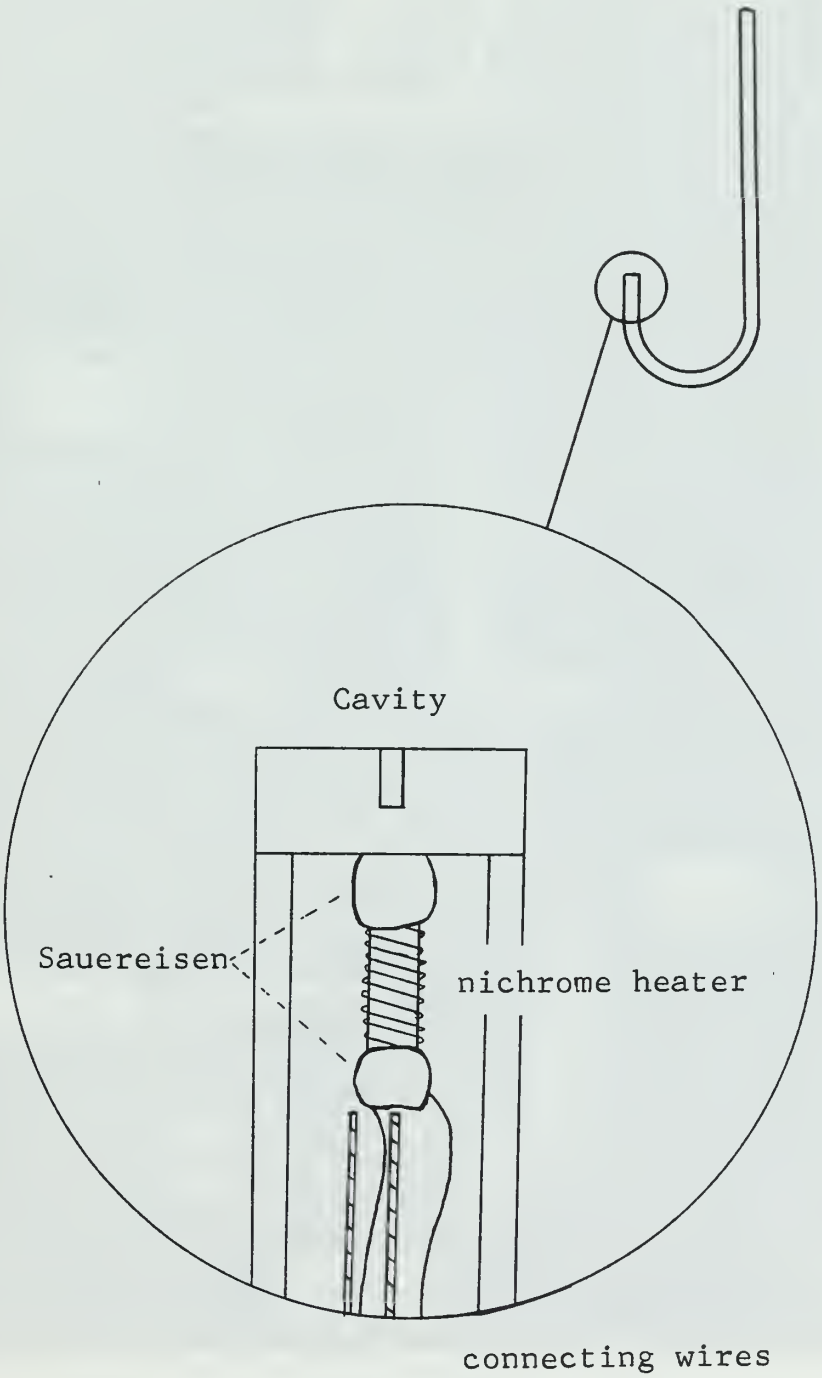

Fig. 2. - Heated Capillary Construction

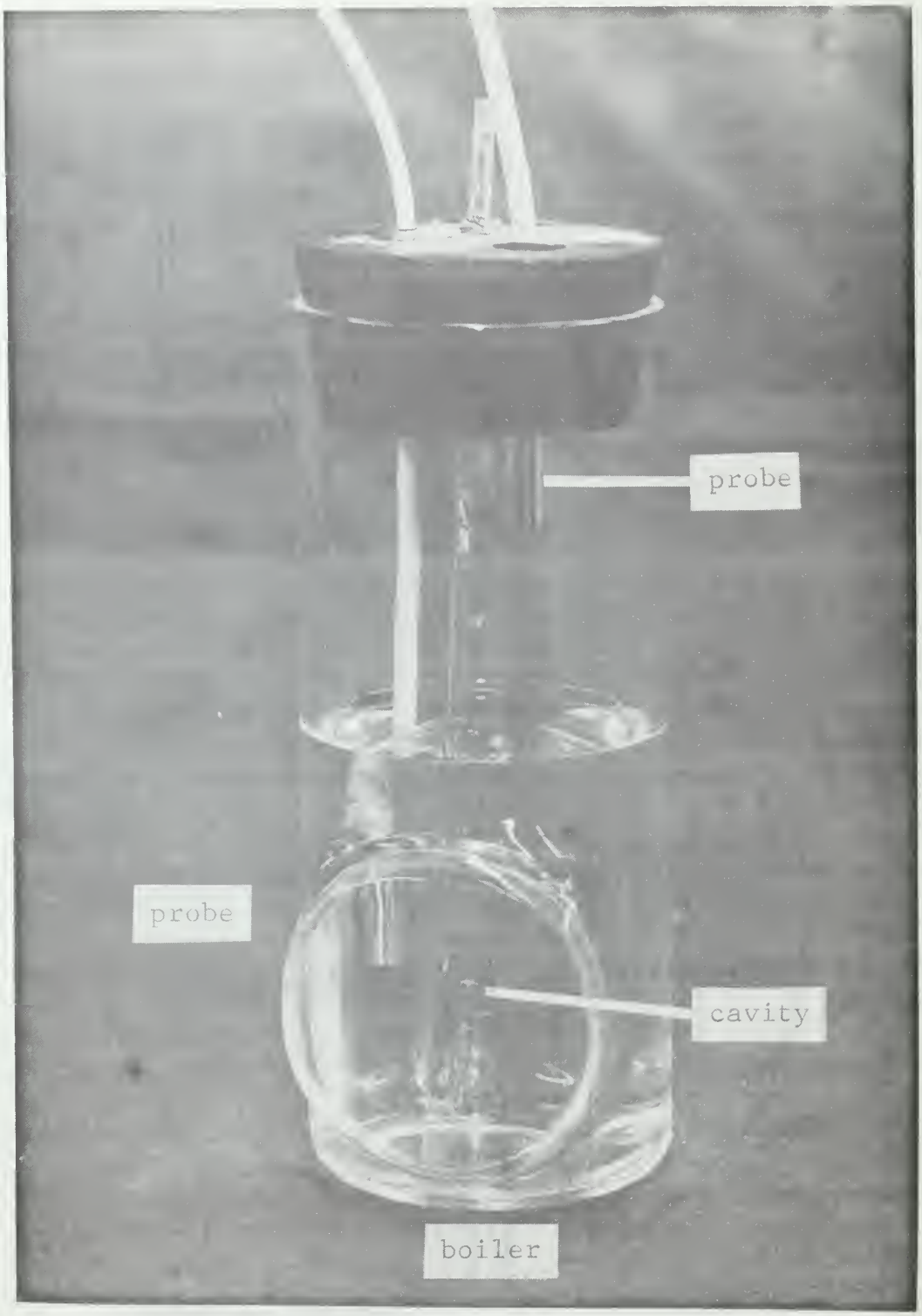

(Full Scale)

Fig. 3. - Photograph of Boiler with Mounted Cavity and Probes

temperature probes. This equipment indicated temperature as a consequence of frequency change by the sensing elements in the probes. Temperature sensitive quartz crystals, the sensing elements in each stainless steel probe, were located parallel to and 0.010 inch from the flat end of the probe. The temperature sensors had a sample period of 0.1 second, resolution of 0.01°C and display interval of 0.2 second. An absolute or differential temperature reading in degrees centigrade could be obtained by proper selection on the front of the cabinet. Accuracy of the combined thermometer probe combination was within $\pm$0.02°C for each measurement. The temperature measurements obtained were assumed within $\pm$0.10°C as a result of actual temperature fluctuations. Each probe lead was inserted in its corresponding split rubber insert and then the assembly was mounted into the large rubber stopper. One probe was positioned in the liquid such that its lower surface was at the same level as the cavity opening but approximately one inch from the cavity. This probe measured the bulk liquid temperature, T_l. The second probe was placed near the top of the boiler in the vapor space. This probe was located 1/2 inch below the rubber stopper to minimize conducted heat through the connecting lead to the probe body and measured the saturation temperature, T_s.

High speed motion pictures were taken through the window of the boiler by using a Fairchild Model HS 401

Motion Analysis Camera. This camera was operated at a nominal film speed of 4800 frames per second by two identical high speed motors. One high speed motor drove the camera's sprocket and the other rotated the take-up spool. The sprocket was geared to turn the rotating prism. The four-faced prism provided the optical compensation by which light received from the lens was directed onto the film at the same rate which the film was moving. The boresight viewfinder was mounted into the camera door and enabled proper focusing of the camera. The sprocket was provided with a 5/16 inch hole to see the film surface while focusing. The surface of the film leader was focused first by rotating the upper barrel on the boresight viewfinder. The subject was then moved into proper position such that the maximum sharpness of object was obtained. The viewfinder was left mounted even during the actual filming, as the subject was checked periodically and again just before actual filming commenced.

Power was supplied to the camera by a Fairchild Model HS-5105B Motor Control. A 30 amp, 115 volt AC source provided sufficient current to operate the rectifier in the Motor Control. An output of 27 volts DC was supplied to the Motion Analysis Camera.

The camera was mounted on a Fairchild Model HS-2511 tripod so that the camera could be raised or lowered, turned about a vertical axis, or elevation angle changed for proper focusing.

The lens system was manufactured using microscope objectives for magnification. The adjusting barrel was machined from aluminum rod. This lens gave a magnification of 3.00 power and magnification could be varied to meet other requirements.

Lighting was supplied by a Colortran Light Fixture with a 1000 watt, very narrow spotlight. The light was placed 18 inches behind the boiler and shone directly through the boiler and cavity into the camera lens. A variac was used to vary the voltage to the light source. A setting of 30 volts was used which provided adequate illumination.

Eastman 4-X, 16MM, Black and White, Panchromatic Negative Film was used for the experimental runs. A 200 foot leader of exposed film was spliced to 200 feet of unexposed film to enable the camera to attain steady operating speed before actual filming commenced.

A General Radio Company, Strobotac, Type 1531A, stroboscope was used to place timing marks on the film. The stroboscope was calibrated before use according to instructions and was operated at a setting of 24,000 flashes per minute. Accuracy was stated by the manufacturer to be within $\pm$ 1% after calibration. The timing marks could be read within $\pm$ 1%, thus time measurements were accurate to within $\pm$ 1.4%.

An Eastman Kodak, Model BP-16AR, 16MM, Analyst, movie projector was used to project the films for analysis. This

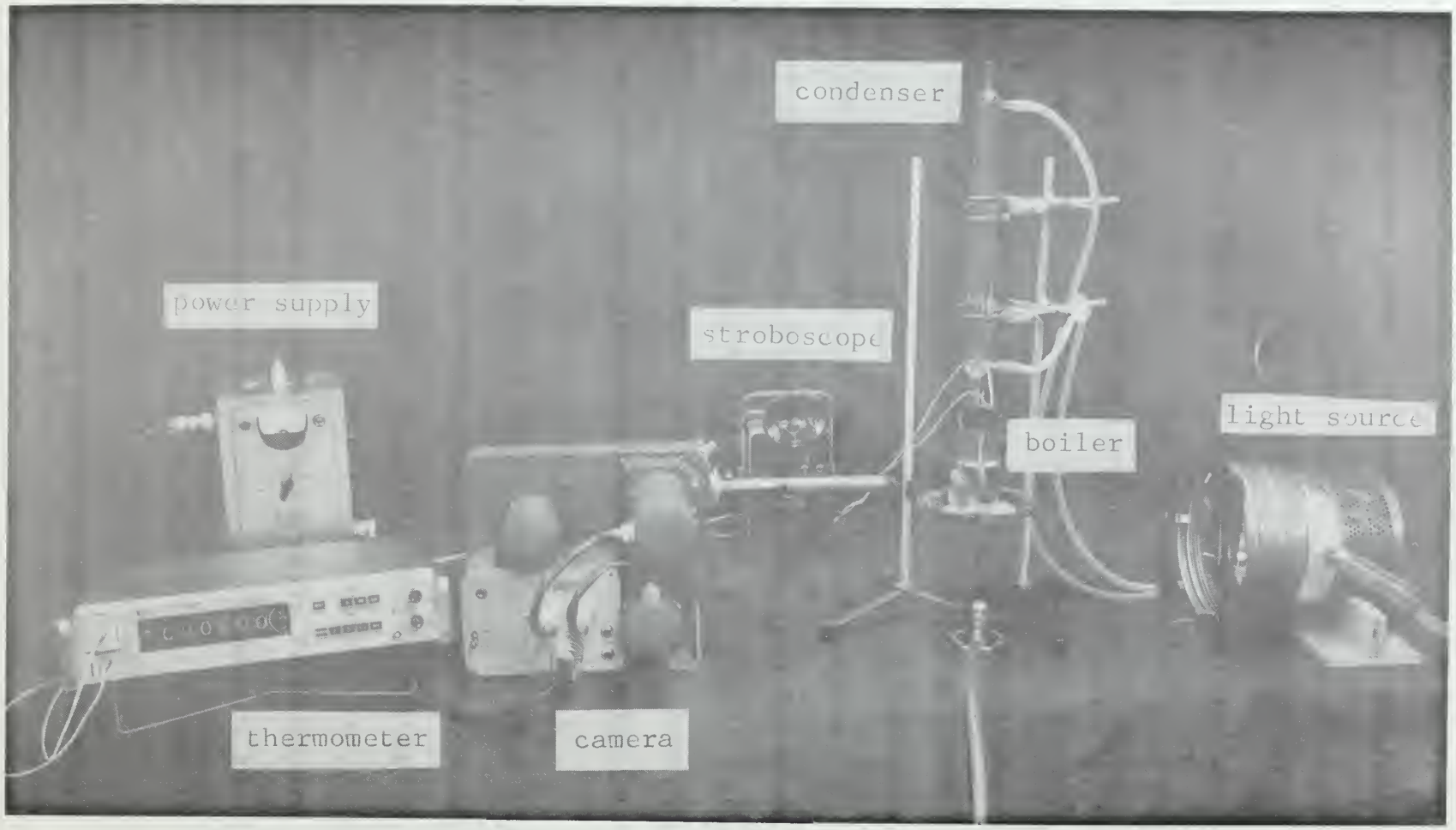

Fig. 4. - Relative Layout of Equipment

projector had an attached frame counter and controls to allow single frame advancement, forward or backwards, or continuous operation in either direction.

A relative layout of equipment setup is shown in Fig.4.

B. EXPERIMENTAL PROCEDURES

The boiler was cleaned before each series of similar runs in an ultrasonic cleaner for 15 minutes. The cleaner used was a commercial alkaline powder and water solution. Upon completion of this procedure, the boiler was flushed with cold tap water, rinsed and filled with distilled water. Sparkleen, a detergent used to clean laboratory glassware, was added and the solution allowed to heat for 30 minutes. The boiler was again rinsed with distilled water and filled to a fixed level with the test fluid. A hypodermic needle used in flusing the cavities was similarly cleaned. Prior to ultrasonic cleaning, the interior of the cavities was scrubbed with synthetic bristles from a paint brush. The cavities were checked to ensure being filled with tap water, then the capillaries were inserted into the ultrasonic cleaner for 15 minutes. Next, the capillaries and cavities were flushed with cold tap water. A distilled water rinse was accomplished on the cavities by employing the cleaned hypodermic needle. The needle was inserted and flushed the cavity with distilled water. The needle was again used to remove residual liquid just prior to mounting in the rubber stopper.

When not in use the cavities were kept in a separate clean boiler filled with distilled water to reduce contamination from particles in the air.

A chromic-sulphuric acid cleaning procedure was also used for comparison. This acid solution was allowed to heat in the boiler and cavities for one hour. The acid was then removed and the boiler and cavities flushed with distilled water. The boiler was immediately filled with distilled water and the cavities mounted in place.

After inserting the cavities into rubber stopper and mounting this assembly in the boiler, fluid was added to the boiler. The mouth of each cavity was located 1 3/4 inches below the surface of the liquid and this depth to the cavity was checked before filming commenced. Cooling water was then circulated through the condenser and heat was applied to the boiler. The fluid was allowed to heat and boil for 20 minutes prior to the actual filming sequence. The light was turned on and the camera focused. The control switch was momentarily depressed and caused the camera to run until all the film went through the camera. The end-of-film switch actuator arm was thus released and the switch automatically cut off power to the camera drive motors. During the camera operation, the strobe light was held above the camera and the light aimed to put timing pips near the edges of the film. Two aluminum tubes were manufactured and inserted into the camera to provide a path for the light pips through

the film guide to the film without otherwise leaking into the interior of the camera body.

Five fluids were used: distilled water, water with wetting agent, water with a viscous agent (sucrose), ethanol, and freon-11. It has been shown (Ref.1) that the addition of 0.04% by weight of Cetyltrimethylammonium-Bromide (a conventional wetting agent) to water decreases its surface tension at 25°C from 71.9 dynes/cm. to 32.0 dynes/cm.; thus this fluid was chosen to study the effects of reduced surface tension.

Viscous effects were studied using a 60% by weight solution of sucrose and water. At 25°C, this fluid has a specific gravity of 1.26 and viscosity of 291.5 millipoise as determined by DuBois (Ref.4).

The effect of density was studied by using trichloro-monofluoromethane, CCl_3F (freon-11). This fluid's density is 1.476 gm/cc at 25°C and has a boiling point temperature of 23.77°C as stated in Ref.5.

Thirty data taking runs were made using the various fluids and cavity geometries. For each run, the following data were taken:

(a) outside diameter of capillary

(b) penetration distance as a function of time, $x(t)$

(c) separation distance, y^*

(d) breakoff angle, α

(e) the number of frames between timing marks at time of departure

(f) number of frames from bubble departure until the interface reached the cavity mouth (n_d)

(d) number of frames from the time the interface reached the cavity mouth until departure of the next bubble (n_g).

C. MEASUREMENT TECHNIQUES

Each roll of film was analyzed by projecting it onto a plane wall. The counter attached to the projector was read to obtain the frame numbers of departure and end of dead time. Outer diameter of each projected capillary was obtained by direct measurement.

The accuracy depended on sharpness of the image and penetration distance. From knowing actual dimensions, a magnification factor was computed. This factor included the effect of the camera lens and also the projector magnification. Interface penetration was measured as the distance from the cavity mouth to the depth at which the liquid-vapor interface was in contact with the wall. In the case of skewed cavities, an average value of penetration was computed from measurements made along both sides. Breakoff distance was measured from the mouth of the cavity to the point at which separation of the vapor bubble occurred. The breakoff angle was measured at the breakoff point and defined as the acute angle of the residual vapor interface as shown in Fig.5. The extension distance, l, was computed as the sum of the breakoff distance and penetration distance. The dead time, t_d, was defined as the

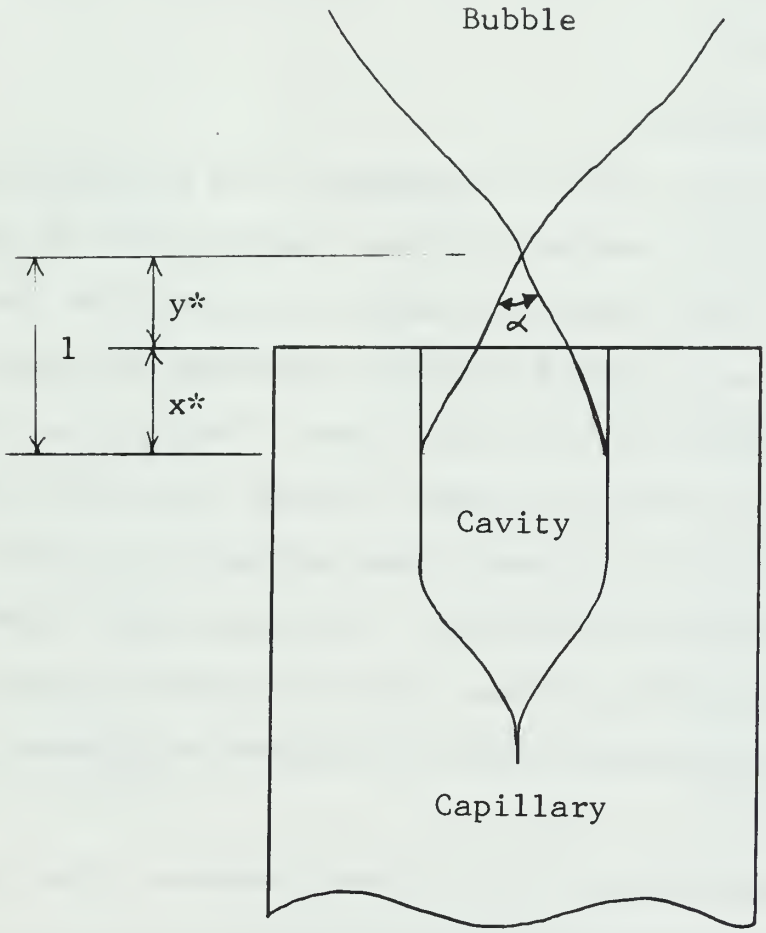

Fig. 5. - Interface Geometry at Bubble Departure

time from bubble departure until the attached interface grew to the cavity mouth. The growth time, t_g, was defined as the time from the end of dead time until departure of succeeding bubble. Both times were calculated from distance measured between timing marks. Bubble frequency was defined as: $f = 1/(t_d + t_g)$ and accuracy determined to be within $\pm 2.8\%$.

D. FILM HANDLING

Each 400 foot roll of unexposed film was first taken into the darkroom and had 200 feet removed onto an empty reel. A 200 foot length of leader, exposed film previously analyzed, was spliced onto the unexposed film and this leader was wound on top of the other. The purpose of this procedure was to run the leader through the camera until the camera reached a steady speed and able to record the rapid motion of the interface. The camera was loaded in darkness but a red light was used to thread the film onto the take-up reel and to check for proper engagement of the sprocket.

Upon completion of the filming sequence, the camera was unloaded in darkness and the reel containing exposed film was placed in a metal film can and taped securely. The camera was then completely checked for film scraps, correct operation, and thus ready to be reloaded for the next run. The exposed film was taken to the darkroom where the leader was removed and attached to another 200

foot length of unexposed film in preparation for other filming runs. All exposed film reels were sent to Photographic Department, Point Mugu, for normal development for this particular type of film.

III. PRESENTATION AND DISCUSSION OF DATA

A. DISCUSSION

1. Growth and Departure of a Typical Bubble

As a result of experimental observations during steady state nucleate boiling, the following description is presented concerning the dynamic growth and departure processes of a typical bubble from a cavity in a J shaped capillary. The sequence of events illustrated in Fig.6 represents a small portion of photographic evidence obtained in this study.

A bubble just departed the cylindrical cavity and the hemispherical liquid-vapor interface was at static equilibrium as shown in Frame 1. Heating caused vaporization from the lower face of the meniscus which forced the liquid out of the cavity and enabled the bubble to grow spherically (Frame 2). Eventually buoyant forces tended to elongate the growing bubble and caused necking down of the vapor at the cavity mouth (Frames 3,4,5). As necking continued, interface contact with the walls moved from the mouth into the cavity (Frames 6 and 7). Penetration distance of the interface into the cavity was almost at a maximum at the time of departure. (Fig.7 represents the penetration curve.) At this instant, the separated bubble accelerated to the surface of the liquid causing a pressure fluctuation in its wake. Due to surface tension

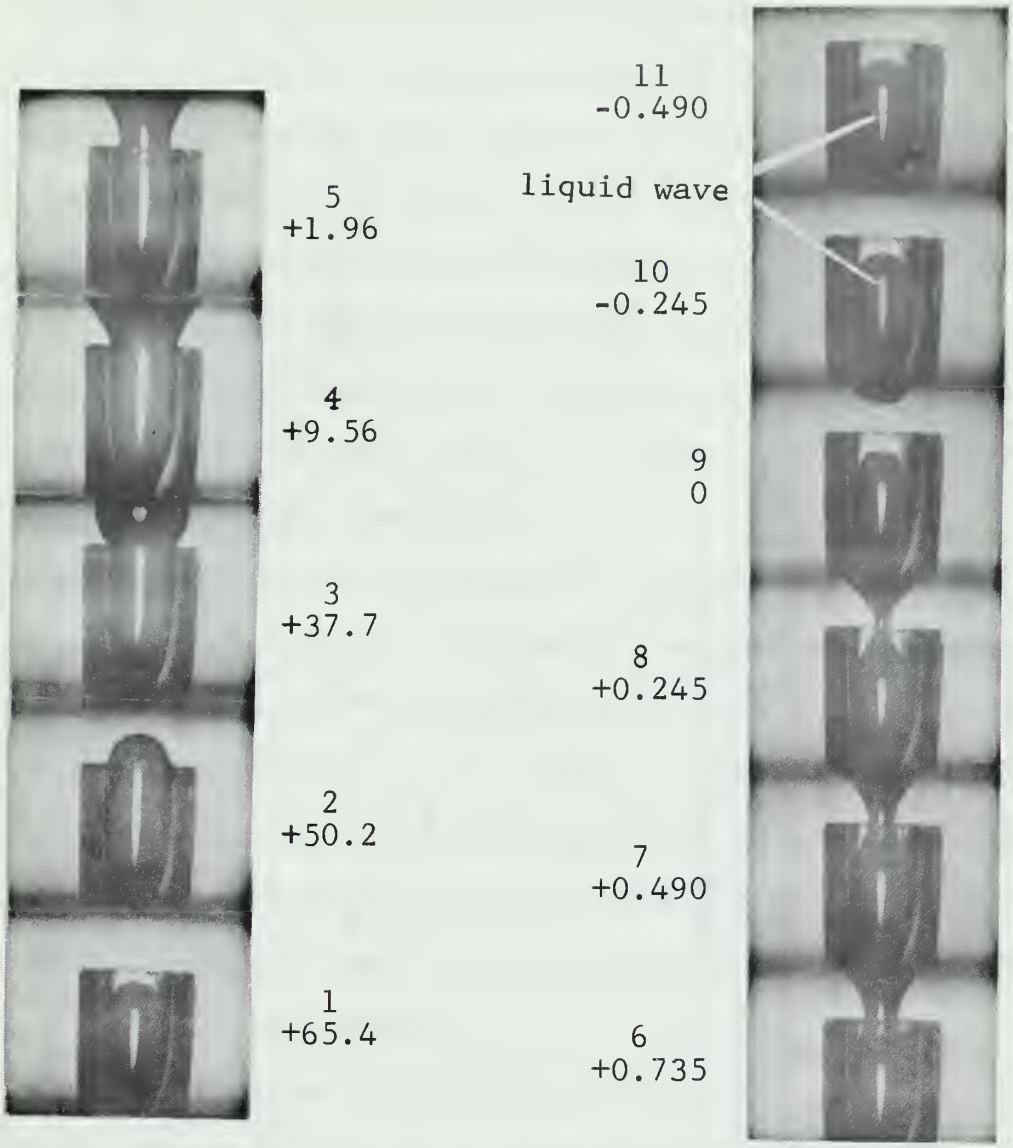

Fig. 6. - Growth and Departure of a Typical Bubble from a Cylindrical Cavity in Water

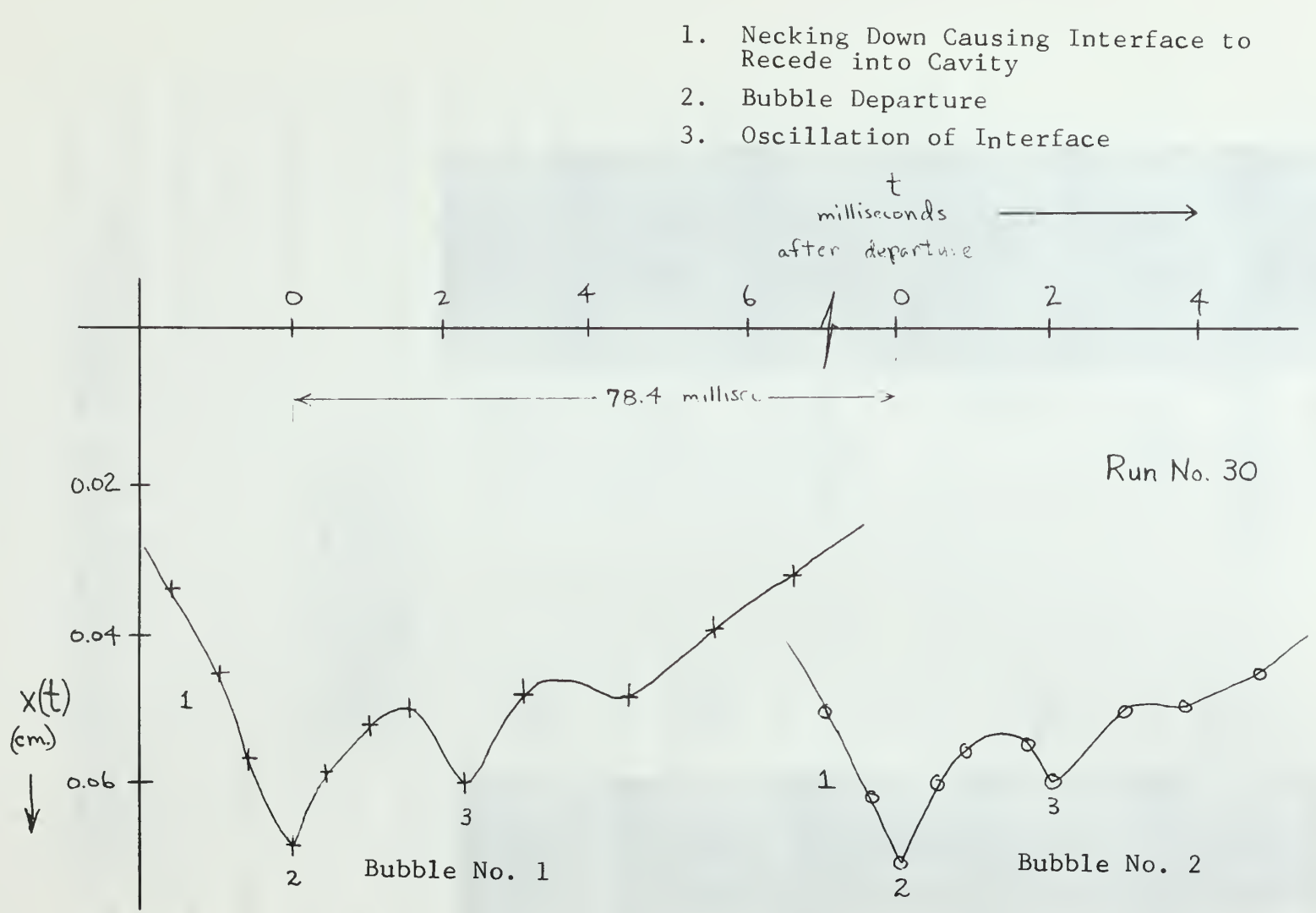

Fig. 7. - Time Behavior of Attached Interface within a Cavity during Several Nucleation Cyles

and pressure forces the residual vapor then collapsed into the cavity where a hemispherical interface was formed. Other forces which may have affected penetration include inertia of liquid as a result of the bubble leaving, and condensation on the liquid vapor interface. Since the vapor bubble accelerates from rest, or nearly so, the inertia force of liquid is small with respect to the pressure forces. Condensation would also have a negligible part due to the great amount of vapor required be condensed to affect penetration.

The superheat required for nucleation to occur is derived in Appendix B. The contact angle was measured to be very close to 0^{o} and for cavity sizes used in this study, a predicted superheat of $0.14^{o}R$ is required for equilibrium. (See Appendix B). Actual superheats in the experimental runs were generally between 1^{o} and $2^{o}C$ which increased the bubble frequency and provided a sufficient amount of bubble cycles recorded on film.

The pressure fluctuation behind the accelerated bubble appeared to deform the residual vapor, especially along the centerline of bubble travel (Frame 9). The side view shows the vapor having a flat surface on top after the bubble has departed, but theory leads to the conclusion that the vapor is depressed in the center, thus appearing as a flat top from the side. The reaction of the residual vapor to this dynamic pressure fluctuation and also to surface tension forces tended to oscillate the interface. The combined

action of the oscillation, surface tension, and dynamic pressure fluctuation forced a thin liquid film down the inner wall of the cavity (Frames 10 and 11). Due to the superheat the liquid film frequently evaporated before reaching the bottom of the cavity, avoiding slugging action. This resulted in reduced dead and growth times.

A liquid slug occurred whenever the film joined together at the bottom of the cavity. This slugging usually filled and deactivated the cavity except when a small amount of trapped vapor grew and forced the slug out. When the volume of the slug was small, as it was being forced out of the cavity, the two hemispherical interfaces came into contact and separated the liquid. This is illustrated in the sequence of events in Fig.8. Surface tension caused the liquid to remain attached to the wall and the liquid flowed down to the bottom to repeat the slugging action. One result of the slugs which were ejected by the trapped vapor was that immediately thereafter, the penetration distance of the next bubble departure was reduced an amount up to 20%. Ensuing penetration increased to a maximum and started to decrease slightly as the liquid slug was being forced towards the mouth of the cavity.

2. Effect of Gravity

A film study of bubble growth and departure from the I shaped capillary produced insight into these processes. Spherical vapor bubbles grew in a similar manner to the cavities whose mouth opened upwards (J shaped

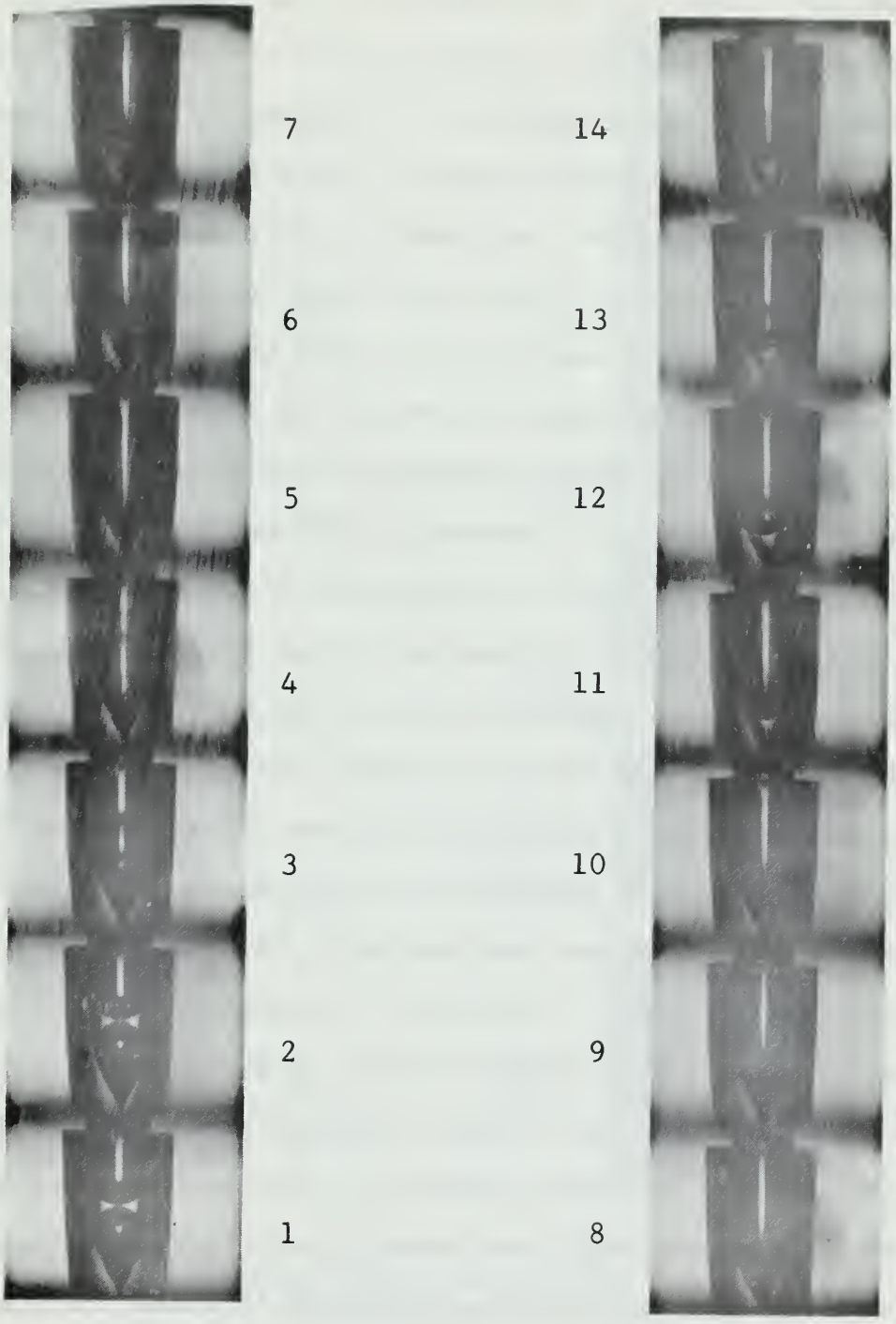

Fig. 8. - Breakup and Formation of Liquid Slug Inside an Operating Cavity

capillaries). (See Fig.9) However in the I capillary, buoyancy effects became noticeable when the bubble diameter approached the outside diameter of the cavity, 0.151 centimeters. The bubble flattened where it was in contact with the submerged surface. When the bubble overlapped or was forced by convection currents to the outer edge of the capillary, the interface made an angle of 28^{o} with the plane of the cavity opening. This angle decreased to a final value of 13^{o} just before the bubble separated from the residual vapor. No liquid film was ever observed on the cavity wall in this case. An important factor in the growth time and hence bubble frequency was the cross sectional surface area of the capillary which served to retain the bubble underneath.

The L shaped capillary, in which the plane of cavity opening was vertical, similarly yielded interesting effects. The vapor bubble grew spherically from the cavity mouth until the bubble diameter approached 0.13 cm when buoyant forces became apparent. (See Fig.9) The bubble continued to grow in size and vertical movement resulted. As the bubble rose an angle of 65^{o} was measured from the top of the cavity mouth to the lower surface of the bubble. Inside the cavity, contact angle was very close to 0^{o} and the angle measured from the vertical to the bubble's lower surface was approximately 35^{o}. There was no liquid film on the inner wall of this cavity. Penetration, measured along the centerline of the cylindrical cavity, was virtually equal to the average of the upper and lower sides.

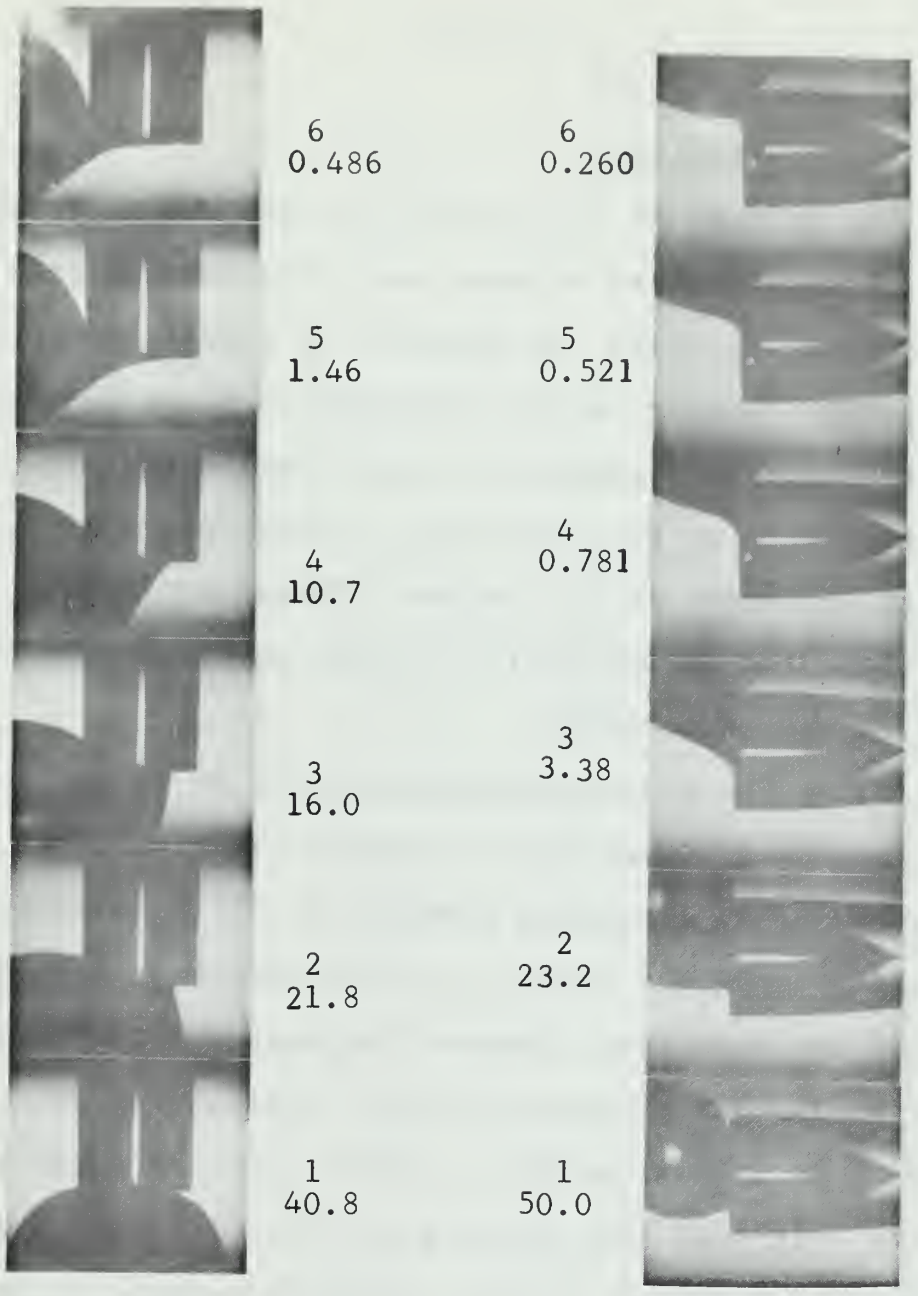

Fig. 9. - Effect of Gravity upon Bubble Growth and Departure from a Cylindrical Cavity in Water

B. PRESENTATION OF DATA

1. Reproducibility

The purpose of this series of runs was to determine how results compare between two different cavities of the same geometry. Also the question of repeatibility of results using the same cavity was hoped to be answered. Table 2 presents data obtained in this series of runs.

A comparison of data obtained in runs 14 and 15 shows good agreement in all values. Therefore results between these two geometrically similar cavities show the validity of reproducibility.

Using the same cylindrical cavity in runs 21 and 27, the results of repeatibility agreed closely. Note that the frequency variation from 2.5 to 5.1 bubbles per second had no apparent effect on the penetration results. Superheat, the difference between the measured temperature of the liquid and the measured vapor temperature, was measured to be approximately the same in run 21 as it was in run 27. Although the accuracy of each probe and lead combination is within $\pm$ 0.02^{o}C, the probe placed in the liquid measured the temperature at the probe's location, not at the cavity. Due to the frequency variation between runs 21 and 27 the local superheat at the cavity may be different than the value measured by the probe.

TABLE 2

Run No.	15	14	27	21
Cavity No.	G-2	G-8	Z	Z
ΔT (degrees C)	1.7	1.8	1.4	1.4
No. Bubbles	7	18	4	9
Liquid Film	Yes	Yes	No	No
Liquid Slugs	Yes	yes	No	No
x^* (cm)	0.079	0.075	0.023	0.025
Accuracy (cm)	$\pm$0.006	$\pm$0.006	$\pm$0.006	$\pm$0.006
$\underline{x}^*$ (cm)	0.009	0.012	0.002	0.006
t_d (sec)	0.011	0.009	0.031	0.015
t_g (sec)	0.088	0.073	0.369	0.182
$t_d + t_g$ (sec)	0.099	0.082	0.400	0.197
f ($\frac{\text{Bubbles}}{\text{sec}}$)	10.1	12.2	2.50	5.08
α (degrees)	60	60	80	75
y^* (cm)	0.007	0.010	0.039	0.038
Accuracy (cm)	$\pm$0.003	$\pm$0.001	$\pm$0.002	$\pm$0.002
l (cm)	0.086	0.085	0.062	0.063
Accuracy (cm)	$\pm$0.009	$\pm$0.007	$\pm$0.008	$\pm$0.008

2. Cleaning Procedure

Table 3 below presents data corresponding to different methods of cleaning the cavities. Runs 14 and 17 employed the detergent cleaner; runs 18 and 19 used the acid cleaning method.

The detergent cleaning method produced greater wettability of the cavities as pointed out by the presence of the liquid film and the slugging action. In runs 14 and 17, the liquid film and slugging increased the liquid surface area and caused a greater evaporation rate than for a cavity with no liquid film. This additional evaporation from the wall surface yielded shorter dead and growth times and therefore higher frequencies than the acid cavities.

The acid cleaned cavities had a greater breakoff distance but a lower frequency due to the decreased wettability. This combination produced smaller extension and penetration distances and a greater departure angle.

These results indicate that penetration appears to be dependent on the wettability of the liquid-solid combination.

3. Superheat

The reentrant cavity, Z, was used to determine the effect of variable superheat. All other conditions remained the same, so that the only variable between successive runs was superheat. Again, superheat was the measured difference between the bulk liquid and liquid saturation

TABLE 3

Cleaning	Detergent	Detergent	Acid	Acid
Run No.	14	17	18	19
Cavity No.	G-8	G-8	G-8	G-2
ΔT (degrees C)	1.8	1.8	2.0	2.0
No. Bubbles	18	13	12	5
Liquid Film	Yes	Yes	No	No
Liquid Slugs	Yes	Yes	No	No
x^* (cm)	0.075	0.069	0.010	0.029
Accuracy (cm)	$\pm$0.006	$\pm$0.001	$\pm$0.002	$\pm$0.002
$\underline{x}^*$ (cm)	0.012	0.017	0.017	0.002
t_d (sec)	0.009	0.005	0.030	0.018
t_g (sec)	0.073	0.067	0.188	0.129
t_d+t_g(sec)	0.082	0.072	0.218	0.147
f ($\frac{\text{Bubbles}}{\text{sec}}$)	12.2	14.0	4.60	6.83
α (degrees)	60	60	80	80
y^* (cm)	0.010	0.011	0.033	0.023
Accuracy (cm)	$\pm$0.001	$\pm$0.003	$\pm$0.001	$\pm$0.001
l (cm)	0.085	0.080	0.044	0.051
Accuracy (cm)	$\pm$0.007	$\pm$0.004	$\pm$0.003	$\pm$0.003

temperature in the vapor space. The liquid temperature was measured at the level of the cavity opening but the probe was located one inch from the cavity. The vapor was assumed to be at the saturation temperature. The local superheat at cavity mouth was not obtained. A listing of data obtained is presented in Table 4.

Results indicate that for the range of superheat obtained in these runs, the bubble frequency was the only parameter which varied. It changed from 2.50 to 8.06 bubbles per second. Other resulting effects may become apparent for greater superheat variation of the liquid and for local superheat variation at the cavity mouth, but no other effects were noticed in these cases for the cavity.

4. Fluids

In this series of runs the objective was to change one fluid physical property at a time and determine its effect. A relationship between the property and results could then be obtained. Data is presented in Table 5. Appendix C includes a tabulation of physical properties of the fluids.

In a comparison between water and water with wetting agent it is noticed that the reduced surface tension characteristics of the wetting solution resulted in no liquid film or slugging action being observed, thus longer dead and growth times and reduced frequency. In addition, the reduced surface tension caused a greater departure angle, shorter extension length, and a smaller penetration distance.

TABLE 4

Run No.	27	21	28	26
Cavity No.	Z	Z	Z	Z
ΔT (degrees C)	1.4	1.4	1.7	1.9
No. Bubbles	4	9	10	16
Liquid Film	No	No	No	No
Liquid Slugs	No	No	No	No
x* (cm)	0.023	0.025	0.019	0.032
Accuracy (cm)	$\pm$0.006	$\pm$0.006	$\pm$0.006	$\pm$0.008
$\underline{x}$* (cm)	0.002	0.006	0.003	0.016
t_d (sec)	0.031	0.015	0.016	0.012
t_g (sec)	0.369	0.182	0.151	0.112
t_d+t_g (sec)	0.400	0.197	0.167	0.124
f ($\frac{\text{Bubbles}}{\text{sec}}$)	2.50	5.08	5.99	8.06
α (degrees)	80	75	80	80
y* (cm)	0.039	0.038	0.040	0.038
Accuracy (cm)	$\pm$0.001	$\pm$0.002	$\pm$0.003	$\pm$0.002
l (cm)	0.062	0.063	0.060	0.070
Accuracy (cm)	$\pm$0.007	$\pm$0.008	$\pm$0.009	$\pm$0.010

The relationship between the sucrose solution and water shows that the increased viscosity and density of the sucrose solution inhibited formation of the liquid film and also slugging . Dead and growth times of the sucrose solution were increased, therefore the smaller frequency resulted. The sucrose solution yielded a shorter extension distance, a greater departure angle, and reduced penetration of the interface into the cavity.

Most of the properties of freon and ethanol differ greatly from the corresponding properties of water. As a result it is virtually impossible to relate data obtained to any specific property. It is sufficient to say however, that for boiling with freon and ethanol, the mechnisms of bubble growth and departure were observed to be very much like boiling with water. The data obtained for freon and ethanol is in good agreement with results for water and therefore the same type of behavior exists. The conductivity of pyrex glass at 100^{o}C is 0.59 BTU/hr-ft-^{o}F, which is greater than the conductivity of water (0.39), ethanol (0.105), or freon (0.05) at their boiling point. Since a similar conductivity relationship exists between actual boilers and fluids, it follows that the same mechanisms for bubble growth and departure occur in actual boiler-fluid combinations.

TABLE 5

Fluid	Water	Wetting Solution	Sucrose Solution	Freon	Ethanol
Run No.	30	37	38	40	41
Cavity No.	52	52	52	52	52
ΔT(degrees C)	2.1	1.1	0.0	1.2	2.9
No. Bubbles	20	5	3	2	7
Liquid Film	Yes	No	No	Yes	Yes
Liquid Slugs	No	No	No	No	No
x^*(cm)	0.074	0.007	0.009	0.068	0.048
Accuracy(cm)	$\pm$0.009	$\pm$0.002	$\pm$0.002	$\pm$0.003	$\pm$0.002
$\underline{x}^*$(cm)	0.003	0.001	0.001	0.001	0.003
t_d(sec)	0.014	0.024	0.033	0.120	0.031
t_g(sec)	0.085	0.331	0.483	0.660	0.181
t_d+t_g(sec)	0.099	0.355	0.516	0.780	0.212
f($\frac{\text{Bubbles}}{\text{sec}}$)	10.1	2.82	1.94	1.28	4.71
α(degrees)	65	85	85	80	80
y^*(cm)	0.004	0.043	0.046	0.016	0.014
Accuracy(cm)	$\pm$0.002	$\pm$0.002	$\pm$0.002	$\pm$0.008	$\pm$0.002
l(cm)	0.078	0 050	0.054	0.084	0.062
Accuracy(cm)	$\pm$0.011	$\pm$0.004	$\pm$0.004	$\pm$0.011	$\pm$0.004

5. Cavity Geometry

Results of variable cavity geometry runs appear in Table 6.

a. L/ID Ratio

A comparison of the runs with the short, cylindrical cavities (runs 8,14,and 15) shows that the slugging action gives faster growth, greater penetration and the breakoff distance is less. For runs 8,29, and 30, which had no slugging action, as the L/ID ratio increased, penetration also increased. Breakoff distance decreased but the extension distance remained constant, hence penetration distance appeared to be related to the internal volume. It is believed that the increased interface penetration was due to the compressibility of the trapped vapor.

b. Cylindrical Cavity Versus Cylindrical-Reentrant Cavity

This comparison shows that the greater internal volume of the cylindrical-reentrant cavity produced greater penetration and greater extension distance, in agreement with results in the L/ID runs.

c. Cavity Geometry

In these runs, the reentrant cavity allowed less penetration than either the conical or cylindrical cavity. Although this does not confirm the compressibility idea of trapped vapor, it must be realized that necking down and breakoff characteristics were changed as a result of the different cavity mouth shapes. DuBois (Ref.4) used ethanol and obtained no measureable penetration for his

TABLE 6

Geometry	L/ID						Cyl.	Cyl. Reent.	Reent.	Cyl.	Con.
	2.72	2.89	2.86	5.15	5.15	8.36					
Run No.	8	15	14	9	29	30	4	5	27	15	22
Cavity No.	10	G-2	G-8	43	43	52	K	24	Z	G-2	4
ΔT(degrees C)	2.2	1.7	1.8	2.1	2.2	2.1	1.8	1.8	1.4	1.7	1.1
No. Bubbles	12	7	18	18	20	20	11	9	4	7	5
Liquid Film	Yes	Yes	Yes	Yes	Yes	Yes	Yes	Yes	No	Yes	No
Liquid Slugs	No	Yes	Yes	Yes	No	No	No	No	No	Yes	No
x^*(cm)	0.059	0.079	0.075	0.073	0.065	0.074	0.058	0.086	0.023	0.079	0.042
Accuracy(cm)	±0.003	±0.006	±0.006	±0.006	±0.006	±0.009	±0.001	±0.001	±0.006	±0.006	±0.006
$\underline{x}^*$(cm)	0.004	0.009	0.012	0.014	0.023	0.003	0.003	0.012	0.002	0.009	0.006
t_d(sec)	0.019	0.011	0.009	0.004	0.007	0.014	0.023	0.040	0.031	0.011	0.052
t_g(sec)	0.113	0.088	0.073	0.061	0.074	0.085	0.125	0.167	0.369	0.088	0.292
t_d+t_g(sec)	0.132	0.099	0.082	0.065	0.081	0.099	0.148	0.207	0.400	0.099	0.344
$f(\frac{\text{Bubbles}}{\text{sec}})$	7.54	10.1	12.2	15.4	12.4	10.1	6.75	4.84	2.50	10.1	2.91
α(degrees)	55	60	60	60	65	65	65	65	80	60	80
y^*(cm)	0.020	0.010	0.007	0.012	0.014	0.004	-0.006	-0.009	0.039	0.007	0.016
Accuracy(cm)	±0.002	±0.003	±0.001	±0.002	±0.003	±0.002	±0.002	±0.003	±0.002	±0.003	±0.002
l(cm)	0.078	0.089	0.082	0.085	0.078	0.078	0.053	0.077	0.062	0.086	0.058
Accuracy(cm)	±0.005	±0.009	±0.007	±0.008	±0.009	±0.011	±0.003	±0.004	±0.009	±0.009	±0.008

reentrant cavity, but the conical cavity allowed a much greater penetration (0.0204 in.) than the cylindrical cavity (0.0039 in.). Using ethanol, Eller (Ref.6) obtained 0.0177 in. penetration in his conical cavity, 0.0181 in. for reentrant cavity, and 0.0251 in. for his cylindrical cavity. In water, Eller arrived at a penetration of 0.0339 in. for conical, 0.0146 in. for cylindrical, and 0.0024 in. for his reentrant cavity. It is emphasized that cavity depth in these previous studies was not constant and their results should be considered in this light.

6. Operating Conditions

The results of various operating conditions appear in Table 7.

a. Gravity

In the Discussion section the effect of gravity was explained concerning the mechanisms of bubble growth and departure. To summarize for this section, the basic effect of gravity is to change the bubble dynamics and therefore departure and penetration.

b. Heat Flux

Comparing runs 32 and 33, it is observed that as heat flux was increased, frequency increased greatly, extension distance decreased slightly, and penetration remained fairly constant. Data obtained during run 34 falls between the values for the other power settings and does not agree with the above mentioned

trend. In run 34, it is believed that the increased power to the heater resulted in greater thermal radiation losses so that less heat was actually conducted to the cavity walls. Also it must be kept in mind that the addition of heat may have raised the local capillary temperature and changed the fluid properties.

c. Pressure

In runs 41 and 42, the pressure was decreased from atmospheric to 8.0"Hg vacuum. The decrease in pressure increased penetration and extension distances. We may reason that the decrease in pressure caused the liquid saturation temperature to decrease and the latent heat of vaporization to increase. Since the heat supplied to the boiler remained constant, a reduced bubble frequency resulted.

TABLE 7

	Shape			Heat Flux(Watts)			Pressure(in.Hg Vac.)	
	J	L	I	0.0	11.08	18.28	0.0	8.0
Run No.	15	13	12	32	33	34	41	42
Cavity No.	G-2	G-2	G-8	32	32	32	52	52
ΔT(degrees C)	1.7	1.1	1.8	2.0	1.9	1.8	2.9	1.7
No.Bubbles	7	13	5	10	14	15	7	5
Liquid Film	Yes	No	No	No	No	No	Yes	Yes
Liquid Slugs	Yes	No	No	No	No	No	No	No
x*(cm)	0.079	0.033	0.003	0.048	0.048	0.048	0.048	0.067
Accuracy(cm)	$\pm$0.006	$\pm$0.002	$\pm$0.001	$\pm$0.003	$\pm$0.004	$\pm$0.004	$\pm$0.002	$\pm$0.002
$\underline{x}$*(cm)	0.009	0.003	0.001	0.002	0.002	0.003	0.001	0.002
t_d(sec)	0.011	0.026	0.016	0.029	0.003	0.003	0.031	0.043
t_g(sec)	0.088	0.132	0.262	0.169	0.033	0.047	0.181	0.291
t_d+t_g(sec)	0.099	0.158	0.278	0.198	0.036	0.050	0.212	0.334
f($\frac{\text{Bubbles}}{\text{sec}}$)	10.1	6.35	3.60	5.06	27.6	20.0	4.71	2.98
α(degrees)				65	70	70	80	80
y*(cm)				0.037	0.022	0.025	0.014	0.006
Accuracy(cm)				$\pm$0.003	$\pm$0.004	$\pm$0.004	$\pm$0.002	$\pm$0.001
l(cm)				0.085	0.070	0.073	0.062	0.073
Accuracy(cm)				$\pm$0.006	$\pm$0.009	$\pm$0.008	$\pm$0.004	$\pm$0.003

IV. CONCLUSIONS

1. For the J shaped capillaries with cylindrical cavities, after bubble departure, a thin liquid film travels down the inner wall of the cavity. If the film evaporates before reaching the bottom of the cavity, then the cavity remains active. On the other hand, if the liquid film reaches the bottom of the cavity, a liquid slug forms, deactivating the cavity.

2. In studying interface behavior during bubble nucleation, consistent results can be obtained for geometrically similar cavities and for the same cavity at different times, provided care is exercised in the cleaning procedure.

3. Penetration by the liquid-vapor interface is influenced by surface tension, viscosity, and wettability of the liquid.

4. Cavity mouth geometry as well as internal volume influences penetration.

5. The effect of heat flux and superheat is to change frequency, but not the penetration.

6. There is greater penetration at lower pressures.

7. Bubble departure dynamics, including the necking down process, influences penetration.

V. RECOMMENDATIONS FOR FUTURE WORK

To better understand the variables affecting nucleate boiling, the following is recommended:

1. Investigate the liquid film on the cavity wall which either evaporates or reaches the bottom of the cavity.

2. Obtain greater variations in pressure and superheat.

3. Investigate variations of local superheat at the cavity mouth.

4. Study the effects of various cleaning methods for the cavities and the boiler.

APPENDIX A

CAVITY CONSTRUCTION

The construction of the glass cavities, which served as models of actual nucleation sites, involved maintaining close tolerances on all dimensions. In order to compare data systematically one dimension was varied at a time to obtain experimental results from which qualitative relationships could be deduced.

A glass blowing lathe was used to mount and rotate the cavities while properly applying heat from a gas fire. Sufficient heat was applied to seal the capillary and shape the cavity as desired. For example, by heating for a short time, the glass walls contracted to form a re-entrant cavity. The glass was cut on a carborundum wheel and ground to form a flat squared-off end.

The heated cavity was used to obtain an internal heat flux effect. The body was first constructed from an 8 mm Pyrex rod drawn so that a cylindrical 0.2 cm by 2.3 cm tip extended from the body.

A nichrome wire of 0.0079 centimeters diameter, 11.60 cm length and 2.35 ohms/cm resistance was used as the heater element. Copper lead-in wires were soldered to each end of the nichrome heater. The heater was then carefully wrapped around the extended glass tip and Sauereisen, a commercial, powdered, electrical cement, which served as

a conductor of heat but an insulator of electricity, was applied at each end to bond the heater in position against the glass.

An 0.8 cm glass tube was slipped over the lead-in wires, down over the mounted heater, and ring sealed to the glass rod. The rod was cut 0.3 cm from the seal and ground to square the end. By heating the flat end and applying a tungsten needle, a cavity was formed, followed by a final grinding to true the surface.

One copper lead-in wire was encased by a glass capillary to prevent electrical shorting. The tubing assembly was next bent into the shape of a J to allow the cavity to open upwards.

APPENDIX B

SUPERHEAT REQUIRED FOR NUCLEATION

For a liquid in contact with its own vapor at equilibrium, certain conditions must hold:

a. Both phases must be at uniform temperatures

b. Chemical potentials must be equal in both phases

c. For a spherical liquid-vapor interface (assuming 0^{o} contact angle of the liquid on the cavity wall)

$$p_v - p_l = \frac{2\sigma}{r} \tag{B-1}$$

or

$$\frac{p_v}{p_l} = 1 + \frac{2\sigma}{p_l r} \tag{B-2}$$

In a liquid, the Clapeyron equation

$$\frac{dp}{dT} = \frac{h_{fg}}{T(v_v - v_l)} \tag{B-3}$$

may be simplified, since $v_v >> v_l$. Employing the perfect gas law, this becomes

$$\frac{dp}{dT} = \frac{h_{fg}}{Tv_v} = \frac{ph_{fg}}{RT^2} \tag{B-4}$$

Integrating

$$-\int_{p_1}^{p_v} \frac{dp}{p} = \frac{h_{fg}}{R}\int_{T_s}^{T_v} \frac{dT}{T^2} \qquad \text{(B-5)}$$

which yields

$$\ln \frac{p_v}{p_1} = \frac{h_{fg}}{R}\left(\frac{1}{T_s} - \frac{1}{T_v}\right) = \frac{h_{fg}}{R}\left(\frac{T_v - T_s}{T_v T_s}\right) \qquad \text{(B-6)}$$

Substituting equation (B-1) into (B-6) gives

$$\ln\left(1 + \frac{2\sigma}{p_1 r}\right) = \frac{h_{fg}}{R}\left(\frac{T_v - T_s}{T_v T_s}\right) \qquad \text{(B-7)}$$

Upon rearranging equation (B-7), it yields

$$T_v - T_s = \frac{\frac{T_s^2 R}{h_{fg}} \ln\left(1 + \frac{2\sigma}{p_1 r}\right)}{1 - \frac{T_s R}{h_{fg}} \ln\left(1 + \frac{2\sigma}{p_1 r}\right)} \qquad \text{(B-8)}$$

For a cylindrical cavity in water:

$$T_s = 212^{o}F = 671.7^{o}R$$

$$R_{vapor} = 85.775 \ \frac{ft - lb}{lb - {}^{o}R}$$

$$\sigma = 0.0041 \ lb/ft$$

$$h_{fg} = 7.55 \times 10^{5} \ ft - lb/lb$$

$$p_l = 14.7 + \frac{(1.75)(62.4)}{1728} = 14.76 \text{ lb/in}^2 = 2126 \text{ lb/ft}^2$$

$$r = 0.042 \text{ cm} = 0.00139 \text{ ft}$$

The denominator on the right hand side of equation (B-8) is thus

$$1 - \frac{(671.7)(85.775)}{7.55 \times 10^5} \ln \left[1 + \frac{0.0082}{(2126)(0.00139)} \right] \qquad \text{(B-9)}$$

Simplifying, equation (B-9) becomes

$$1 - 0.00212 = 0.99788 \qquad \text{(B-10)}$$

This value is obtained for the denominator of the right hand side of equation (B-8). Its effect is negligible as the numerator is of the order of unity. Therefore equation (B-8) may be approximated by

$$T_v - T_s = \frac{T_s^2 R}{h_{fg}} \ln \left(1 + \frac{2\sigma}{p_l r}\right) \qquad \text{(B-11)}$$

For an assumed 0^o contact angle

$$p_v - p_l = \frac{2(0.0041)}{0.00139} = 5.90 \text{ lb/ft}^2 = 0.0410 \text{ lb/in}^2$$

$$T_v - T_s = 0.142^oR$$

For contact angle of 30^{o}

$$p_v - p_l = 0.0354 \ lb/in^2$$

$$T_v - T_s = 0.166^{o}R$$

For $2.00^{o}R$ superheat ($T_v - T_s = 2.00^{o}R$)

$$r = 9.74 \times 10^{-5} \ ft = 0.00319 \ cm$$

Equation (B-11) represents an approximate expression for the superheat required at equilibrium of a bubble with radius r. Nuclei of radius greater than r should become bubbles and grow, those of smaller radius should collapse.

APPENDIX C

TABULATION OF PHYSICAL PROPERTIES

Property	Temp.(°C)	Water	Water & Wetting Agent	Water & Sucrose	Ethanol	Freon-11
Density (gm/cc)	25	0.997	0.997(c)	1.28112		1.476(b)
	78	0.973			0.7398(e)	
	100	0.9584	0.9584(c)	1.232(f)		
Surface Tension ($dynes/cm$)	25	71.97	32(g)	76.23(e)		22(b)
	78	63.0(d)			17.74(e)	
	100	58.9	26.2(f)	62.4(f)		
Viscosity (Millipoise)	25	8.904		291.5(h)		4.2(b)
	78	3.638			4.49(e)	
	100	2.818		92.2(f)		
Observed Boiling Temp.(°C)		100.0	100.0	100.0	78.3	23.77(b)

Notes:

(a) Physical Properties (except freon) obtained from: The Chemical Rubber Co., Handbook of Chemistry and Physics, 50th Edition (1969-1970).

(b) Freon Properties from reference (5)

(c) Assumed Value

(d) Interpolated Value

(e) Extrapolated Value

(f) Calculated Value (ratio with water)

(g) Reference (1)

(h) Reference (4)

BIBLIOGRAPHY

1. American Chemical Society, Contact Angle, Wettability and Adhesion, Advances in Chemistry Series 43, p.31, 1964.

2. Bankoff, S. G., "The Prediction of Surface Temperatures at Incipient Boiling", Chem. Engr. Prog. Symposium Series, Chicago, Ill., 1959.

3. Beck, E. J., "Nucleation of Steam Bubbles from Large-Diameter Prepared Sites", U.S. Naval Civil Engineering Laboratory Technical Report R 600, Oct. 1968.

4. DuBois, D. R., "Photographic Investigation of Bubble Nucleation from Glass Capillary Tubes", M.S. Thesis, Naval Postgraduate School, Monterey, California,1967.

5. DuPont DeNemours and Co., Freon Technical Bulletin, 1964.

6. Eller, J. C., "A Photographic Investigation of Bubble Nucleation from Artificial Cavities", M.S. Thesis, Naval Postgraduate School, Monterey, Calif., 1968.

7. Jameson, G. J., and Kupferberg, A., "Pressure Behind a Bubble Accelerating from Rest: Simple Theory and Applications", Chem. Engr. Science, 22, 1053 (1967).

8. Kosky, P. G., "Bubble Growth Measurements in Uniformly Superheated Liquids", Chem. Engr. Science, 23, 695 (1968).

9. Kosky, P. G., "Nucleation Site Instability in Nucleate Boiling", Int. J. Heat Mass Transfer, 11, 929 (1968).

10. Marto, P. J., and Rohsenow, W. M., "Nucleate Boiling Instability of Alkali Metals", Journal of Heat Transfer, 88, Series C, May 1968.

11. Trefethen, L., "Surface Tension in Fluid Mechanics", Fluid Mechanics Film, Dec. 1964.

12. Wei, C. C., and Preckshot, G. W., "Photographic Evidence of Bubble Departure from Capillaries During Boiling", Chem. Engr. Sci., 19, 838, (1964).

INITIAL DISTRIBUTION LIST

		No. Copies
1.	Defense Documentation Center Cameron Station Alexandria, Virginia 22314	20
2.	Library, Code 0212 Naval Postgraduate School Monterey, California 93940	2
3.	Department of Mechanical Engineering Naval Postgraduate School Monterey, California 93940	2
4.	Naval Ship Systems Command Code 2052, Via Code 31 Department of the Navy Washington, D. C. 20360	1
5.	Assoc. Professor Paul J. Marto, Code 59Mx Department of Mechanical Engineering Naval Postgraduate School Monterey, California 93940	3
6.	LT Roger L. Sowersby, USN % Supervisor of Shipbuilding, U. S. Navy Pascagoula, Mississippi 39567	3

UNCLASSIFIED
Security Classification

DOCUMENT CONTROL DATA - R & D

(Security classification of title, body of abstract and indexing annotation must be entered when the overall report is classified)

1 ORIGINATING ACTIVITY (Corporate author)	2a. REPORT SECURITY CLASSIFICATION
Naval Postgraduate School Monterey, California 93940	Unclassified
	2b. GROUP

3 REPORT TITLE

A Photographic Investigation of Bubble Nucleation Characteristics

4 DESCRIPTIVE NOTES (Type of report and, inclusive dates)

Master's Thesis; December 1969

5. AUTHOR(S) (First name, middle initial, last name)

Roger L. Sowersby

6. REPORT DATE	7a. TOTAL NO. OF PAGES	7b. NO. OF REFS
December 1969	66	12

8a. CONTRACT OR GRANT NO.	9a. ORIGINATOR'S REPORT NUMBER(S)
b. PROJECT NO.	
c.	9b. OTHER REPORT NO(S) (Any other numbers that may be assigned this report)
d.	

10. DISTRIBUTION STATEMENT

Distribution of this document is unlimited.

11. SUPPLEMENTARY NOTES	12. SPONSORING MILITARY ACTIVITY
	Naval Postgraduate School Monterey, California 93940

13. ABSTRACT

The characteristics of bubble nucleation, growth, and departure during nucleate boiling were investigated. The liquid-vapor interface motion was analyzed using high speed motion picture photography. The fluids used were: distilled water, water with wetting agent, water with sucrose, ethanol, and freon-11. Cylindrical, conical, and reentrant cavity geometries were employed in addition to J, L, and I shaped capillaries. Cavity inner diameters were fixed at 0.085 centimeters and cavity depth ranged from 0.230 to 0.703 centimeters.

Consistent results were obtained for geometrically similar cavities and for the same cavity at different occasions. A thin liquid film was observed on the cavity inner wall which was directly related to cavity nucleation stability. The liquid-vapor interface penetration was shown to be dependent upon cavity geometry and fluid properties. Frequency, but not penetration, was affected by heat flux and superheat.

DD FORM 1 NOV 65 1473 (PAGE 1)
S/N 0101-807-6811

UNCLASSIFIED
Security Classification

A-31408

14 KEY WORDS	LINK A		LINK B		LINK C	
	ROLE	WT	ROLE	WT	ROLE	WT
High Speed Photography						
Bubble Nucleation						
Bubble Growth Departure						
Glass Cavities						
Cavity Penetration						
Liquid Film						